FERMILAB-CONF-06-296-TD

Development and Test of LARP Technological Quadrupole (TQC) Magnet

S. Feher, R.C. Bossert, G. Ambrosio, N. Andreev, E. Barzi, R. Carcagno, V.S. Kashikhin, V.V. Kashikhin, M.J. Lamm, F. Nobrega, I. Novitski, Yu. Pischalnikov, C. Sylvester, M. Tartaglia, D. Turrioni, R. Yamada, A. Zlobin, S. Caspi, D. Dietderich, G. Sabbi

***Abstract*—In support of the development of a large-aperture Nb_3Sn superconducting quadrupole for the Large Hadron Collider (LHC) luminosity upgrade, two-layer quadrupole models (TQC and TQS) with 90-mm aperture are being constructed at Fermilab and LBNL within the framework of the US LHC Accelerator Research Program (LARP). This paper describes the construction and test of model TQC01. ANSYS calculations of the structure are compared with measurements during construction. Fabrication experience is described and in-process measurements are reported. Test results at 4.5K are presented, including magnet training, current ramp rate studies and magnet quench current . Results of magnetic measurements at helium temperature are also presented.**

***Index Terms*—LARP, LHC, IR, Nb3Sn, quadrupole magnet, collars, yoke, skin.**

I. Introduction

One of the primary objectives of the US LHC Accelerator Research Program is to develop a Nb_3Sn quadrupole for a future LHC upgrade. Models using two different structures [1][2], each using identical coils, are being constructed in collaboration between Lawrence Berkeley Lab (LBNL) and Fermilab (FNAL). The TQC01 structure, developed and built at Fermilab, consists of stainless steel collars surrounding the coils supported by an iron yoke and thick stainless steel skin.

II. Magnet Design and Analysis

A. Magnet Design

The TQ coils (common to TQC and TQS) are manufactured using a 2-layer cos-2θ configuration with a 90mm bore and one wedge in the inner layer. TQC coil and structural design and 2D analysis have been previously discussed [2].

Manuscript received August 29, 2006. This work was supported the U.S. Department of Energy.

S. Feher, R.C. Bossert, G. Ambrosio, N. Andreev, E. Barzi, R. Carcagno, V.S.Kashikhin, V.V. Kashikhin, M.J. Lamm, F. Nobrega, I. Novitski, Yu. Pishalnikov, C. Sylvester, M. Tartaglia, D. Turrione, R. Yamada and A. Zlobin are with Fermi National Accelerator Laboratory, P.O. Box 500, Batavia, Il. USA (corresponding author to provide phone: 630-840-2240; fax: 630-840-xxxx; e-mail: fehers@ fnal.gov).

S. Caspi, D. Dietderich and G. Sabbi are with :Lawrence Berkeley National Laboratory, Berkeley, CA 92740 USA.

B. Instrumentation

TQC01 is instrumented with strain gauges at various positions to measure preloads and stresses within structural components during assembly and testing. Coil instrumentation included azimuthal gauges on the inner coil and axial gauges on the inner surface of the bronze pole pieces, both in the straight section and at the pole on the lead end. Control spacers, skins and end preload bolts (bullets) were also instrumented. Also, shims were placed at specified positions to control coil preload. Fig. 1 shows the TQ structure with the main structural components labeled, and the positions of strain gauges and shims noted. Fig. 2 shows the lead end of a coil with positions of strain gauges shown.

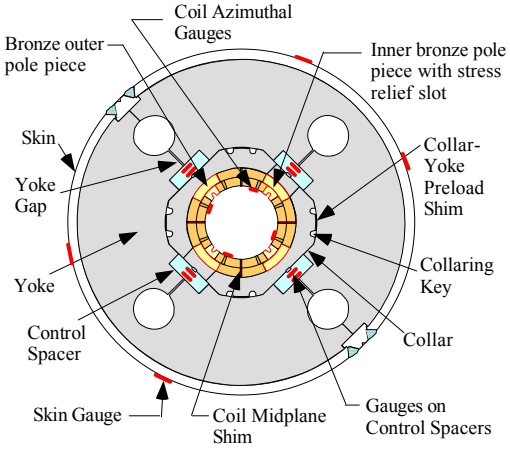

Fig. 1. TQ Structure with Positions of Instrumentation.

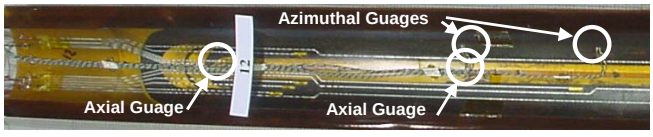

Fig. 2. Inner Surface of Instrumented Coil.

C. Analysis

2D and 3D analysis has been completed [2] [3]. Table 1 shows expected stresses within the structure according to the 2D analysis. End load was chosen based on 3D analysis and previous experience with Nb3Sn dipoles and NbTi quadrupoles at Fermilab.

TABLE 1
EXPECTED STRESSES WITHIN TQC01

Gauges	Units	After keying	After Assembly
Coil Az (peak)	MPa	70	140
Coil Az (at gauges)	MPa	50	100
Cont Sp	MPa		50
Skin	MPa		150
Bullets	KN		14

III. MAGNET FABRICATION

A. Mechanical Models

A series of mechanical models were completed to test the production processes and to compare stresses within the structure to the analysis. A preliminary mechanical model [4] demonstrated that coil azimuthal pre-stress along the magnet length can be controlled to within 15MPa, allowing the keying process to take place without degrading the Nb3Sn cable. The 2nd and 3rd models consisted of collared coils only, and were used to understand coil size and preload levels after collaring, by measuring stresses within the completed collared coil assembly and comparing them to expected values. Moderate variations in preload between coils resulted in the elimination of the "tabbed" collar (used for coil alignment) in favor of a "full round" design for TQC01 as shown in Fig. 3. The tabbed collar may be reintroduced, depending on the results of measurements of coil size variations and the TQC01 test. The final two mechanical models included yokes, and were used to establish the coil mid-plane and collar-yoke shims needed for TQC01. Results indicated similar preload of about 70 MPa in both the inner and outer layers, after keying. Increase in strain of coils during yoke assembly was about a factor of 2, similar to the values derived from the 2D analysis.

Fig. 3. Collar Laminations, 'With Pole Tab" and "Full Round"

B. Magnet Construction

Four coils were wound and cured at Fermilab, reacted and impregnated at LBNL, then shipped back to FNAL, by a process described in [2]. This process has demonstrated that shipment of Nb3Sn coils can be routinely achieved without damage, allowing the two labs to collaborate on Nb3Sn magnet fabrication very efficiently. TQC01 assembly was completed at FNAL. Readings of gauges at various stages of assembly are shown in Table 2.

Assembly begins with coil arrangement, splicing of NbTi leads and application of ground insulation. Collaring and keying is done in a hydraulic press, as shown in Fig. 4. Initial pressure is applied by main cylinders, after which key cylinders are energized. Multiple passes are applied, with key depth controlled and incrementally increased with each pass. TQC01 was keyed twice, first without mid-plane shims and the second time using a 50 μm shim at each coil mid-plane. Inner layer coil azimuthal preload after each keying was determined by strain gauges on coils as shown in Fig. 2 and by collar deflection measurements, shown in Fig. 5. Measurements agree that preload was approximately 70 MPa after keying with a 50 μm mid-plane shim. Collar deflection "low points" appear at the positions where the cable is turning around the ends. "High points" occur where the cross section is made completely of bronze end parts. After completion of the collared coil assembly, TQC01 was yoked and the skin was welded longitudinally at four positions using automatic weld heads. A 425 μm collar-yoke shim was used. Average coil preloads from azimuthal gauges during collaring and yoke welding is shown in Fig. 6. Weld is typically applied in several (4-6) passes, with increasing stress applied to the coils from skin stretching during each pass. The initial two passes yielded higher than expected coil stresses, but in subsequent passes the force from the skin was diverted to the control spacers, as expected from the analysis. Some asymmetry between coils occurred, due to uneven side-to-side application of load by the press, to be corrected with shimming in future assemblies. End plates were installed and total end load of 14 kN was applied to each end by mechanically tightening the end preload bolts (bullets).

TABLE 2
STRESSES WITHIN TQC01 COMPONENTS DURING CONSTRUCTION

Gauges	Units	Position	After Keying	After Assembly
Coil Azimtl	MPa	Q1 (end, ctr)	40, 36	88, 116
Coil Azimtl	MPa	Q2 (end, ctr)	52, 52	68, 108
Coil Azimtl	MPa	Q3 (end, ctr)	18, 32	74, 94
Coil Azimtl	MPa	Q4 (end, ctr)	46, 28	84, 96
Coil Axial	MPa	Avg(end , ctr)	15,15 (tens)	30,30 (tens)
Cont Sp	KN/cm	Average	----------	130
Skin	MPa	Avg near weld	----------	170
Bullets	KN	LE Avg.	----------	14
Bullets	KN	NLE Avg.	----------	14

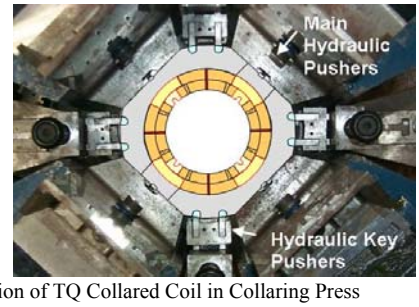

Fig. 4. Illustration of TQ Collared Coil in Collaring Press

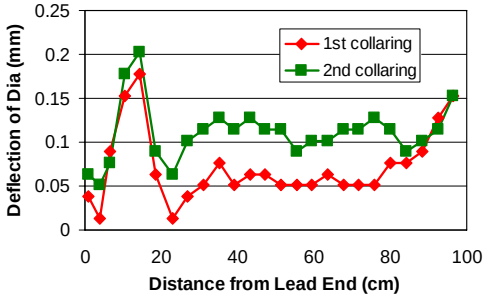

Fig. 5. Collar Deflection Measurements.

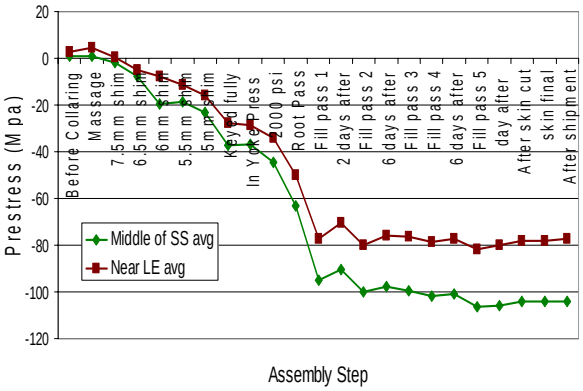

Fig. 6. Coil Azimuthal Stresses during Construction as read by Coil Gauges. (based on coil MOE of 40 GPa)

IV. Test Results

TQC01 was tested in Fermilab's Vertical Magnet Test Facility (VMTF) in August 2006.

A. *Quench Test*

Magnet training was performed in a liquid helium bath at a temperature of 4.5 K. Current ramp rate for training quenches was 20 A/s (see Fig. 7.). The quench current for the first quench was only 7681 A, about 60% percent of the estimated critical current value of the conductor. The magnet exhibited very slow training, reaching 8995 A after 11 quenches, still only 70% of the critical current limit. Quench current did not significantly increase over the next five quenches, even falling back 3 times.

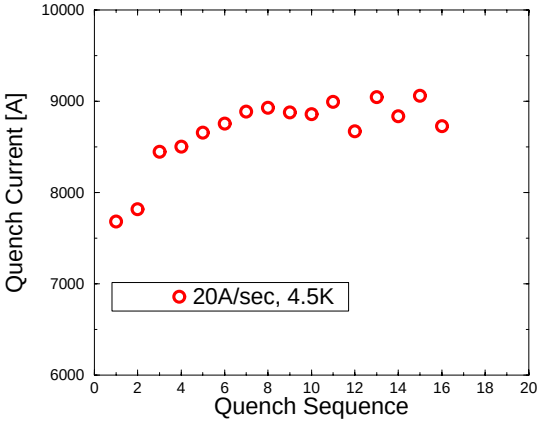

Fig. 7. TQC01 Training Curve. The magnet critical current limit is 12900A.

Quench locations for all of the 20 A/s quenches were in the pole turn region of the inner coils, which is the highest field region of the magnet. Longitudinal locations were not concentrated in a particular section of the coils, although no end region quenches were observed (see Fig. 8.).

All training quenches occurred in an area which contained a specific structural feature, which was included as a result of mechanical model tests (see above). The original TQC design implemented a collar lamination which included the pole area of the outer coil, as shown in Figure 3. As a result, the outer pole pieces were not glued in place during impregnation, but instead mold released so they could be removed later. When the design was changed to the "full round" collar, these pieces were left in the structure, but not glued into position. The section nearest the lead end, where the cable transitions from the inner to outer layers, does have the outer pole piece glued into place. All the quenches in TQC01 (with the possible exception of no. 8) have occurred in the area which includes outer pole pieces that are not glued, represented by the area enclosed by dotted lines in Fig. 8.

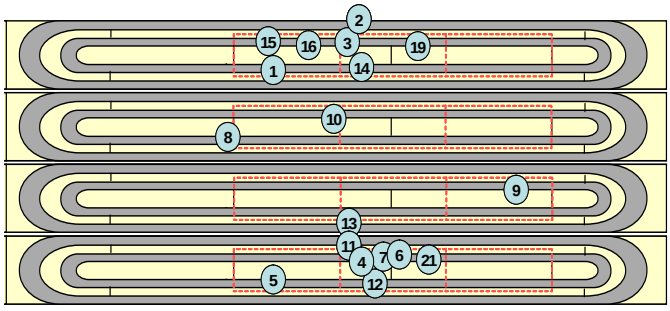

Fig. 8 TQC01 Quench Positions at 4.5K Figure is shown looking at the inside surface of the inner coils, with the lead end on the left and Quadrants 1 through 4 positioned from top to bottom. (Ramp rate quenches 19 and 21 have been added because they were done at a rate less than 175 A/s and occurred in the inner coil pole turn.)

Magnet training was followed by quench current ramp rate dependence studies (see Fig. 9.). The quench current ramp rate dependence is flat between 0 and 175 A/s, then continuously decreases with increasing ramp rate. This ramp rate dependence behavior is a clear indication that the quench current limitation is not related to conductor damage. Locations of quenches with higher than 175A/sec ramp rate were in the mid-plane section of the inner coil, whereas the 175 A/sec and lower ramp rate quenches occurred in the pole turn region of the inner coil.

The fact that the training quenches occurred only in the high field region, coupled with the high RRR value (250) of the coils and relatively slow quench propagation velocities (~10 m/s), indicates that conductor instability is not the primary cause of the quench current limitation. More likely, the limitation is caused by inadequate mechanical support of the coils.

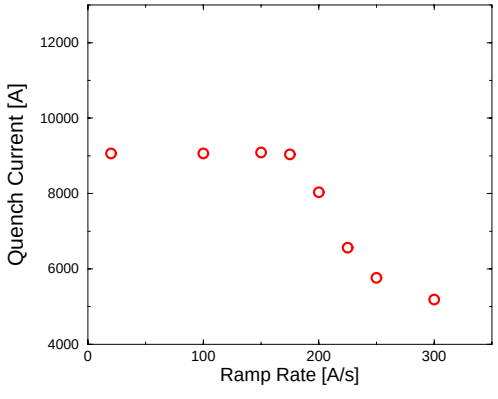

Fig. 9. TQC01 Quench Current Ramp Rate Dependence.

The absence of cable degradation indicates that the collaring process described above has been successfully completed without degrading the Nb_3Sn conductor. TQC01 is the first Nb3Sn magnet to be built with the collaring and keying process used traditionally for NbTi magnets at Fermilab [5]. Since the magnet is keyed incrementally (in 8 cm segments), differential pressure between segments during the keying process, and the possible cable degradation created by it, was considered an issue that needed to be resolved by the TQC01 assembly.

B. *Strain gauge results*

1) Cool-down: All strain gauges were read during cool-down and excitation. Strain gauges mounted to the skin showed increasing stress during cool-down, as expected by the analysis. Load on control spacers increased during cool-down, as expected, taking the load from the skin without transferring it to the coils. Azimuthal coil preload during cool-down decreased somewhat, a behavior not expected by the analysis, which indicated that preload should have been about the same after cool-down as at room temperature. End preload bolts stayed in contact with the coils at 4.5 K, with the amount of force remaining flat or increasing slightly. Axial gauges on the bronze inner poles, in tension at room temperature, showed a decrease in tension when cold.

2) Excitation: During excitation, skin stresses remained flat as expected. Stress in control spacers decreased slightly under the Lorenz forces, indicating that azimuthal load was being transferred from the control spacers to the coil mid-planes, as expected. This behavior revealed that at the 9000 A force level (about half of the designed value at full current), the yoke and skin structural rigidity is consistent with the analysis.

Adequate end support was confirmed by bullet gauges. The increase in end load under the Lorenz forces was about 15% of the level calculated for total end force from Lorenz forces. This shows that the coil axial support through radial force from the collar, yoke and skin structure is utilized. Also, as Lorenz forces began to increase, load increased immediately and linearly, indicating that the ends remained loaded at all times.

Azimuthal gauges showed unloading of the coils close to 9000 A (Fig. 10). This indicates that the azimuthal pre-stress of the coils was not sufficient. Low pre-stress might be a reason for the poor training behavior of the magnet. Also, strong asymmetrical loading with current appears near the center of the magnet. This phenomenon is less pronounced in the end area where the outer pole is glued. Detailed mechanical analysis of the magnet will be presented later.

C. *Magnetic measurements*

Magnetic measurements were also performed. Harmonic measurements are summarized in Table 3. It is important to notice that the presence of a relatively large a3 is another indication that the coils are asymmetric, which could be related to their uneven preload.

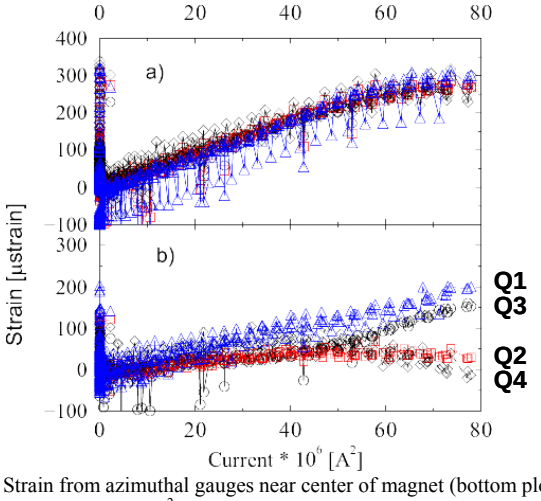

Fig. 10. Strain from azimuthal gauges near center of magnet (bottom plot) and near lead end (top plot) vs. I^2.

TABLE 3
MEASURED HARMONICS OF TQC01 AT 4.5K, 6.5 KA

	Units		Units
b3	-0.05	a3	-3.37
b4	-0.79	a4	-0.02
b5	0.17	a5	-0.18
b6	-0.14	a6	-0.02
b7	0.02	a7	-0.06
b8	0.03	a8	-0.02
b9	0.06	a9	0.00
b10	0.04	a10	0.03

V. CONCLUSION

TQC01, the first Technology Quadrupole in a series of 2-layer Nb_3Sn quadrupoles for LARP, has been completed. Construction steps were performed successfully, with most parameters during construction in agreement with the mechanical analysis. Testing is still taking place, but preliminary data from quench behavior, strain gauges and harmonic measurements indicate problems with mechanical support. Results of testing will be analyzed and used to improve performance in subsequent TQC magnets.

REFERENCES

[1] S. Caspi, et al.., "Design and construction of TQS01, a 90mm Nb3Sn Quadrupole Model for LHC Luminosity Upgrade Based on a Key and Bladder Structure," in *IEEE Transactions on Applied Superconductivity*, Vol. 16, No 2, pp. 358-361, June 2006.

[2] R. C. Bossert, et al., "Development of TQC01, a 90mm Nb3Sn Model Quadrupole for LHC Upgrade Based on SS Collar," in *IEEE Transactions on Applied Superconductivity*, Vol. 16, No 2, pp. 370-373, June 2006.

[3] Wands, Bob, *TQ 3D Mechanical Analysis"*, Fermilab Technical Division Technical Memo TD-06-046.

[4] Tavano, Giuseppe, *TQ Mechanical Model Initial Results"*, Fermilab Technical Division Technical Memo TD-05-042.

[5] R. C. Bossert, et al., "Construction Experience with MQXB Quadrupole Magnets built at Fermilab for the LHC Interaction Regions," in *IEEE Transactions on Applied Superconductivity*, Vol. 13, No 2, pp. 1297-1300, June 2003.